Preparation and Electro-optical Behaviors of Polymer Stabilized Liquid Crystal Cells with Chiral Matrices Derived from (−)-Camphor

Jui-Hsiang Liu,[1] Hsien-Jung Hung,[2] Dung-Shin Wu,[2] Shou-Mau Hong,[2] Andy Y. G. Fu[3]

[1]*Department of Chemical Engineering, and Institute of Electro-optics, National Cheng Kung University, Tainan, 70101, Taiwan*
[2]*Department of Chemical Engineering, National Cheng Kung University, Tainan, 70101, Taiwan*
[3]*Department of Physics, and Institute of Electro-optics, National Cheng Kung University, Tainan, 70101, Taiwan*

Received 5 May 2004; accepted 28 December 2004
DOI 10.1002/app.22032
Published online in Wiley InterScience (www.interscience.wiley.com).

ABSTRACT: Novel chiral monomers derived from (−)-camphor and difunctional monomers with biphenyl segments were synthesized. The molecular structures were identified using FTIR, NMR, and elemental analyses. Surface pretreated polymer stabilized cholesteric texture (PSCT) cells with various chiral nematic components were prepared. According to theory, they are kind of reversed mode PSCT cells. The helical twisting power (HTP) and pitches of the PSCT cells were evaluated. The polarized optical microscopic (POM) textures and the dependence of the optical properties on the applied voltage of the PSCT cells were investigated. The reflection band of the PSCT cells before and after UV irradiation were estimated. A blue shift of selective reflection of the PSCT cells was obtained after UV irradiation. PSCT cells with various reflecting colors and the dependence of the transmittance of the cells on applied voltage were investigated. Real image recording through a mask as well as the transmittance of PSCT cells controlled by applied voltage were also confirmed. © 2005 Wiley Periodicals, Inc. J Appl Polym Sci 98: 88–96, 2005

Key words: synthesis; UV–vis spectroscopy; crosslinking; monomers; phase separation

INTRODUCTION

Cholesteric liquid crystals exhibit two stable states at zero field: the reflecting planar texture and the nonreflecting (scattering) focal conic texture. Their optical properties, such as color and reflectivity, are important in display and image duplicating applications.[1–8] When a cholesteric liquid crystal is in the planar texture, there is a periodic structure of the refractive index in the cell's normal direction. The refractive index oscillates between the ordinary refractive index n_o and the extraordinary refractive index n_e. The period is $P_o/2$ because n and –n are equivalent. The liquid crystal exhibits Bragg reflection at the wavelength $\lambda_o = 2n(P_o/2) = nP_o$ for normally incident light. The reflection peak is broad and has a bandwidth given by ΔnP_o, where $\Delta n = n_e - n_o$ is the birefringence. The maximum reflection of an unpolarized normally incident light from the cholesteric liquid crystal is 50%. 100% reflection can be achieved by stacking a left-handed cholesteric liquid crystal and a right-handed cholesteric liquid crystal film.[9,10] Since the reflected wavelength $\Delta\lambda$ is only a part of the visible wavelength, a colored reflected light can be seen. The reflective optical properties can be used for the recording of color images.

It is well known that azobenzene undergoes isomerization from trans to cis under ultraviolet light irradiation, while the cis form can return to the trans form either photochemically or thermally. Such geometrical change could produce a concomitant change in physical and chemical properties not only in the azobenzene itself but also in the surrounding matrices. When the azobenzene is embedded in nematic liquid crystal, the two isomers produce different environments, which are characterized by the two different molecular shapes. The rod-like rigid molecule of the trans form is favorable for the stabilization of the liquid crystal phase, while the bent cis isomer tends to destabilize the phase structure. Therefore, the ordered nematic phase is isothermally transformable into a disordered isotropic phase by the trans–cis photoisomerization of the guest azobenzene. The photochemical phase transition of liquid crystals has been examined conveniently by the transmission and reflection mode analyses.[11–15]

From such a viewpoint, the light scattering mode control of light was proposed and accomplished by employing a polymer matrix combined with the liquid crystal system in lieu of the function of polarizers,

Correspondence to: J.-H. Liu (jhliu@mail.ncku.edu.tw).

similar to a polymer stabilized cholesteric texture (PSCT).[3,16,17] In general, the light scattering state is operated through electrical control of the ordering of the liquid crystal domains as in other liquid crystal devices. PSCTs with a memory function, which are potential for image storage and laser addressed displays, were also reported.[18–21] In these composite films, optical information can be recorded due to a reversible change in threshold frequency induced by isomerization of azobenzene.

In our previous study, we reported optical control of the light through the polymer/liquid crystal composite film based on the control of the electric field.[22,23] In the system, phase separation of polymers in liquid crystal leads to the formation of focal-conic texture domains. In case of an absence of an electric field, the focal-conic structure is formed and caused by the light scattering phenomena. When an electric field is applied to the PSCT cells, the direction of liquid crystals reorients parallel to the direction of the applied field, and the PSCT cells become transparent.

To fabricate and characterize reversed PSCT cells with chiral monomers and chiral nematic liquid crystal mixtures, the novel monomeric bornyl 4-(6-Acryloyloxyhexyloxy) phenyl-4′-benzoate (BAPB), derived from (−)-camphor, and the difunctional monomeric 4,4′-bis(6-acryloyxy-hexyloxy)biphenyl (BAHB) were synthesized. Polarized optical microscopic (POM) texture and the UV–vis spectra of the PSCT cells fabricated in this investigation were studied. Real image recording and optical properties of the PSCT cells were estimated.

EXPERIMENTAL

Measurements

^{1}H NMR spectra were recorded on a Bruker AC-200 NMR spectrometer. Infrared spectra were measured by a Jasco 410 spectrometer in the range 4000–400 cm^{-1} and collected at 4cm^{-1} resolution. The optical rotation of chiral compounds was measured with a Jasco DIP-370 using the D-line of sodium (λ = 589nm). Measurements were performed using 1% solutions of substances in THF. Differential scanning calorimeter (DSC) was conducted with a Perkin–Elmer DSC 7 at a heating and cooling rate of 10 K min^{-1} in nitrogen atmosphere. Thermal decomposition temperature data were recorded with a thermogravimetric analyzer (TGA) Perkin–Elmer TGA 7. The phase transitions were investigated by an Olympus BH-2 polarized optical microscope (POM) equipped with Mettler hot stage FP-82, and the temperature scanning rates were determined at a rate of 5 K min^{-1}. Gel permeation chromatography (GPC) was carried out with a Shimadzu C-R4A equipped with a HITACHI L-6000 pump, using THF as the eluent and the rate of the elution was 1.0 mL min^{-1}; the instrument was calibrated with a polystyrene standard. UV spectroscopy measurements were carried out with a Jasco V-550 UV–VIS spectrophotometer. The X-ray diffraction data was recorded on a RIGAKU RINT 2500 series with Ni-filtered CuKα radiation. The sample in a quartz capillary was held in a temperature-controlled cell (RIGAKU LC high-temperature controller).

Materials

Nematic liquid crystal mixture ZLI-2293 and chiral liquid crystal additive CB-15 were purchased from Merck Taiwan Ltd. and used as a host liquid crystal without further purification. Chiral monomer and difunctional monomer were synthesized in this investigation. 4-Hydroxybenzoic acid, 1-chloro-6-hexaol, *N*,*N*′-dimethylaniline, 2,6-di- *tert*-butyl-*p*-cresol, ethyl-4-hydroxybenzoate, and (−)-camphor were all purchased from Wako, Tokyo.

Synthesis of monomers

Synthetic routes for the target monomers are shown in Schemes 1 to 4. The chiral bornyl derived monomers were synthesized according to similar procedures described in the literature.[24,25]

4,4′-bis(6-(acryloyxy)- hexyloxy)biphenyl (BAHB) was synthesized according to the method reported.[23,24]

4-(6-Hydroxyhexyloxy) benzoic acid (**1**)

4-Hydroxybenzoic acid (16.57g, 120mmol) was dissolved in the mixture of EtOH (42 mL) and H_2O (18 mL). KOH (17.8g. 317.8mmol) and a catalytic amount of KI dissolved in EtOH (50 mL) was added dropwise to the solution. 1-Chloro-6-hexaol (22.5g, 165mmol) was then added, and the solution was heated to reflux for 24 h. The resulting mixture was poured into water and extracted with ethyl ether. The water phase solution was acidified with HCl diluted with water until weakly acidic. The resulting precipitate was filtered and washed several times with water. The crude product was recrystallized from EtOH/H_2O (4/1). Yield 19.1g (67%), T_m = 139–140°C. FTIR (cm^{-1}): 3249 (OH), 1685(C═O), 1287, 1251 (C-O-C). ^{1}H NMR DMSO-d_6, δ (ppm): 12.6 (s, 1H, -COOH), 7.9 (d, 2H Ar, ortho to -COOH), 7.0 (d, 2 H, Ar, meta to -COOH), 4.4 (s, 1H, OH), 4.0 (t, 2H, -CH_2OPh-), 3.4 (t, 2H, -CH_2-OH), 1.28–1.74 (m, 8H).

4-(Acryloyloxyhexyloxy) benzoic acid (**2**)

Compound (**1**) (7.15g, 31.5mmol), N,*N*-dimethylaniline (4g, 33.0mmol), and a catalytic amount of 2,6-Di-*tert*-butyl-*p*-cresol was dissolved in distilled 1,4-dioxane (50 mL). The solution was cooled with an ice/salt bath, and then acryloyl chloride (9 mL, 99.3mmol) dissolved in distilled 1, 4-dioxane (20 mL) was added

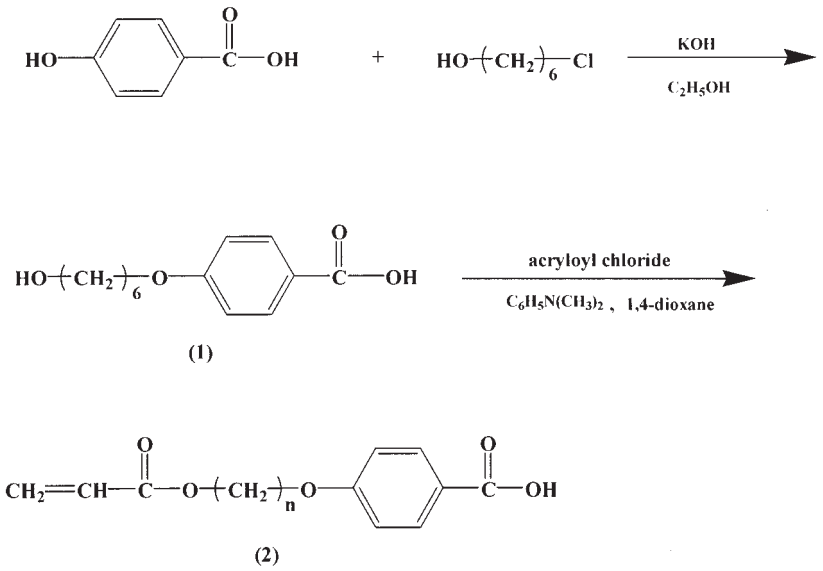

Scheme 1

dropwise under vigorous stirring. After completing a 24 h reaction at room temperature, the solution was poured into cold water and the precipitate was filtered. The crude product was washed several times with water and recrystallized twice from EtOH. Yield 6.3g (69%), K 88°C N 92°C I. FTIR (cm $^{-1}$): 2945, 2864 (CH_2), 1725 (C═O), 1604, 1291, 1246 (C-O-C), 1675 (C═C). ^{1}H NMR, $CDCl_3$, δ (ppm): 12.5 (s, 1H, -COOH), 8.0 (d, 2H, Ar, ortho to –COOH), 7.0 (d, 2H, Ar, meta to -COOH), 5.8, 6.4, 6.1 (s, 3H, H_2C═ CH-), 4.1 (t, 2H, -$COOCH_2$-), 4.0 (t, 2H, -CH_2OPh-), 0.94–1.28 (m, 8H, -CH_2-).

Ethyl 4-(tetrahydro-2-pyranyloxy) benzoate (**3**)

Ethyl 4-hydroxybenzoate (25 g, 150.6 mmol) was dissolved in CH_2Cl_2 (200 mL) with a catalytic amount of *p*-toluene sulfonic acid (*p*-TSA) at 30°C. 3, 4-Dihydro-2H-pyran (37.9 g, 451.8 mmol) was added dropwise, and the solution was then stirred for 24 h. The reaction mixture was washed with 5% aqueous $NaHCO_3$ and water, dried over $MgSO_4$, and evaporated. The white powder was recrystallized twice from EtOH, yield 23.7g (63%). FTIR (cm^{-1}): 2941, 2867 (CH_2), 1684 (C═O in Ar-COO-), 1601, 1498 (C-C in Ar), 1290, 1244 (COC). ^{1}H NMR ($CDCl_3$, δ = ppm): 1.25–1.86 (m, 9H, methyl), 3.59 (m, 1H, OCH_2CH_2), 3.83 (m, 1H, OCH_2CH_2), 4.33 (q, 2H, OCH_2CH_3), 5.47 (m, 1H, O$CH$$CH_2O$), 7.05 ~ 7.97 (m, 4H, aromatic).

4-(Tetrahydro-2-pyranyloxy) benzoic acid (**4**)

Compound 3 (23.0 g, 92.0 mmol) was dissolved in THF (100 mL). KOH (15.4 g, 276.0 mmol) dissolved in MeOH/water (7/1, 100 mL) was added to the former solution and then heated at reflux for 24 h. After the

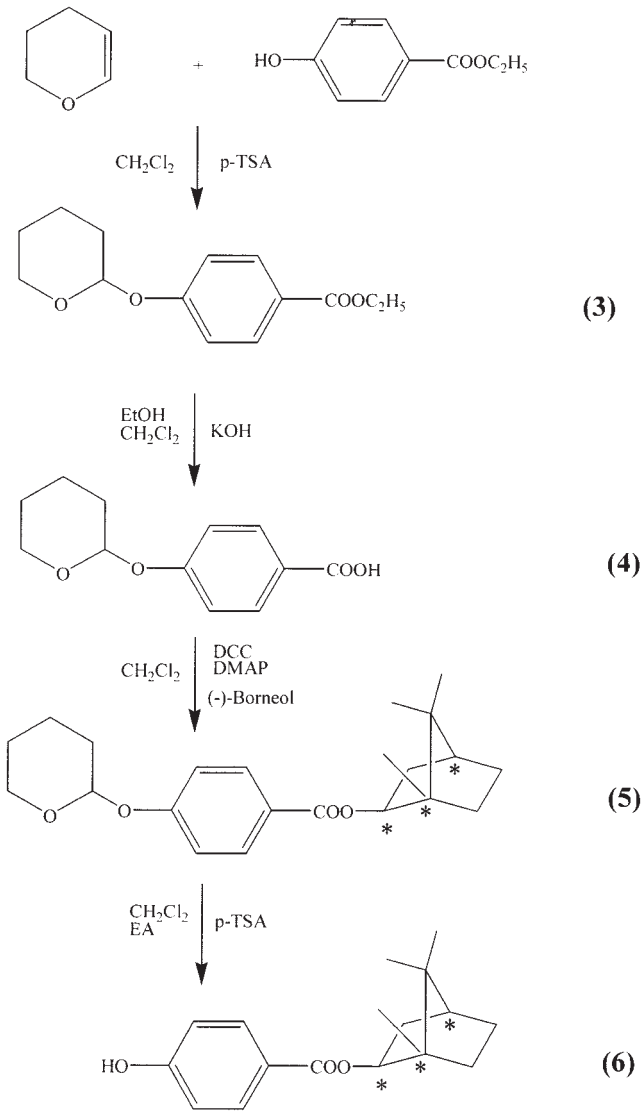

Scheme 2

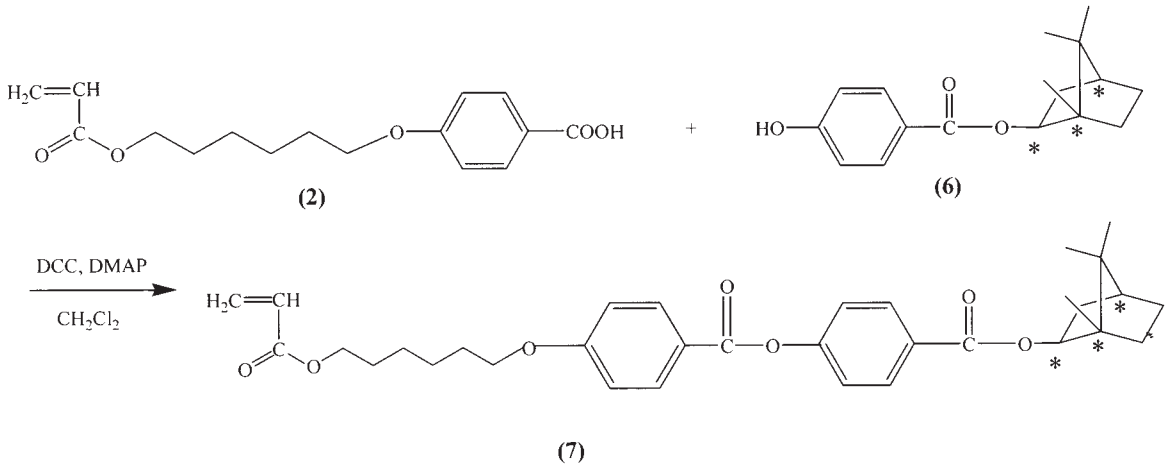

(2) (6) (7)

Scheme 3

reaction, the THF was removed. The resulting suspension was poured into water and neutralized with diluted HCl to pH = 5. The resulting precipitate was filtered and washed with water several times, and recrystallized twice from EtOH/H_2O (6/1). Yield 15.1 g (74%), T_m = 199–200°C. FTIR (cm^{-1}): 2945, 2873 (CH_2), 1674 (C═O in Ar-COO-), 1608, 1505 (C-C in Ar), 1278, 1244 (COC), 2663, 2540 (COOH). ^1H NMR (acetone-d6, δ = ppm): 1.65–1.83 (m, 6H, methyl), 3.59 (m, 1H, OC$H_2$$CH_2$), 3.79 (m, 1H, OC$H_2$$CH_2$), 5.56 (m, 1H, OC$H$$CH_2O$), 7.11 ~ 7.97 (d, 4H, aromatic).

Bornyl 4-(tetrahydro-2-pyranyloxy) benzoate (**5**)

Compound 4 (14.5 g, 65.3 mmol) and (−)-Borneol (10.2 g, 65.3 mmol) were dissolved in CH_2Cl_2 (100 mL) at 30°C. N,N′-dicyclohexyl- carbodiimide (DCC) (40.7 g, 195.9 mmol) and N,N′-dimethyl-aminopyridine (DMAP) (0.7 g, 6.5 mmol) were dissolved in CH_2Cl_2 (50 mL) and then added to the former solution, and stirred for 2 days at 30°C. The resulting solution was filtered and washed with water, dried over $MgSO_4$, and evaporated. The

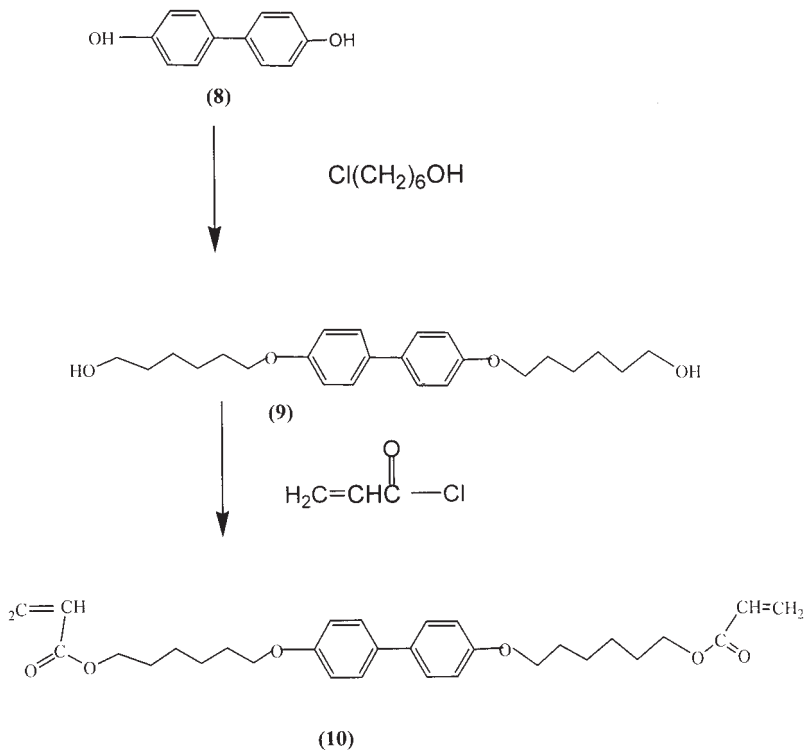

(8) (9) (10)

Scheme 4

crude product was purified by column chromatography (silica gel, ethyl acetate/hexane = 1/6), and then recrystallized twice from EtOH, yield 10.9 g (47%). FTIR (cm^{-1}): 2950, 2873 (CH_2), 1710 (C═O in Ar-COO-), 1608, 1510 (C-C in Ar), 1275, 1244 (COC). ^1H NMR ($CDCl_3$, δ = ppm): 0.89–2.45 (m, 22H, methyl), 3.61 (m, 1H, OCH_2CH_2), 3.84 (m, 1H, OCH_2CH_2), 5.07 (q, 1H, OCHCH_2O), 5.49 (m, 1H, OCHCH_2), 7.07 ~ 8.00 (m, 4H, aromatic).

Bornyl 4-hydroxybenzoate (**6**)

Compound **5** (10.2 g, 28.4 mmol) was dissolved in CH_2Cl_2/MeOH (1 : 1, 60 mL) and a catalytic amount of *p*-TSA was added to the solution. The mixture solution was stirred at 50°C for 12 h, and the solvent was then evaporated. The crude product was purified by column chromatography (silica gel, CH_2Cl_2) and recrystallized twice from EtOH/H_2O (6/1), yield 5.9 g (76%), T_m = 134–135°C. FTIR (cm^{-1}): 3324 (OH), 2960, 2878 (CH_2), 1679 (CO in Ar-COO-), 1613, 1510 (C-C in Ar), 1229, 1280 (COC). ^1H NMR (*d*-acetone, δ = ppm): 0.96–2.42 (m, 16H, methyl), 5.06 (m, 1H, OCHCH_2), 6.90 ~ 7.90 (m, 4H, aromatic).

Bornyl 4-(6-acryloyloxyhexyloxy) phenyl-4′-benzoate (bapb) (**7**)

Compound (**2**) (8.5g, 29.1mmol) and bornyl 4-hydroxybenzoate (6) (7.9g, 29.0mmol) was dissolved in CH_2Cl_2 (100 mL) at 30°C. N,N′-dicyclohexylcarbodiimide (DCC) (18.0g, 87.0mmol) and N,N′-dimethylaminopyridine (DMAP) (0.34g, 2.9mmol) were dissolved in CH_2Cl_2 (50 mL), then added to the former solution and stirred for 2.5 days at 30°C. The resulting solution was filtered and washed with water, dried over $MgSO_4$, and then evaporated. The crude product was purified by column chromatography (silica gel, ethyl acetate/hexane, 1/8) and recrystallized twice from EtOH. Yield 6.1g (39%), T_m = 56°C. The equation and the molecular structures are shown in Scheme 3. IR (cm^{-1}): 2945, 2873 (CH_2), 1741 (CO in Ar-COO-), 1608, 1505 (C-C in Ar), 1198, 1244 (COC), 1710 (CO in Ar-COO-Ar′), 1633 (C═C). ^1H NMR ($CDCl_3$, δ = ppm): 0.93–2.49 (m, 24H), 4.06 (m, 2H), 4.19 (m, 2H), 5.13 (m, 1H), 5.82 (m, 1H), 6.14 (m, 1H), 6.43 (m, 1H), 6.99 (d, 2H), 7.28 (d, 4H), 8.15 (d, 4H).

4,4′-Bis(6-hexyloxy)biphenyl (**9**)

A commercially available 4,4′-dihydroxybiphenyl (**8**) (6.8g, 36.5mmol) was dissolved in a mixture of ethanol (200 mL) and water (40 mL). The mixture was heated to 110°C, potassium hydroxide (4.5g, 80mmol) in ethanol was added, 6-choloro-1-hexanol (5g, in 50 mL ethanol) was further added dropwise. The mixture was heated at reflux for a further 24 h. After completing the reaction, the solvent was evaporated. The residue was washed with water five times and recrystallized with ethanol. Yield = 78%, FTIR (cm^{-1}): 3324 (OH). E.A. $C_{24}H_{34}O_4$ (386) Cald. C74.61 H8.81 O16.58. Found C74.65 H8.78 O 16.61.

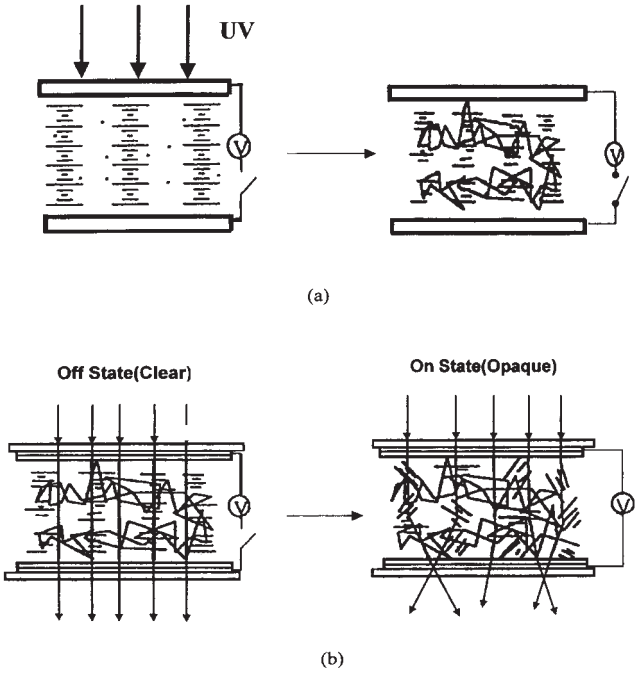

Scheme 5

4,4′-Bis(6-acryloyxy-hexyloxy)biphenyl (BAHB) (**10**)

4,4′-bis(6-hexyloxy)biphenyl (**9**) (5g, 12.75mmol) and n,*n*-dimethyl aniline (6g, 44mmol) in 1,4-dioxane (200 mL) was added to acryloyl chloride (10 mL) and reacted at 25°C for 2 h. The reaction mixture was heated to 55°C; acryloyl chloride (10 mL) was further added and reacted for 24 h. After completing the reaction, the precipitate was filtered and washed with water five times, then recrystallized from ethanol. Yield = 76%, FTIR (cm^{-1}): 1700 (C═O), 1625 (C═C). EA $C_{24}H_{32}O_6$ (494) Cald. C72.88 H7.69 O19.43. Found C72.86 H 7.72 O19.45.

PSCT cell preparation and measurements

The liquid crystal composite cells were prepared from the mixture of ZLI2293/CB15/mono- and difunctional monomers. Since ZLI2293 is a kind of nematic liquid crystal mixture, the composition is very complicated. For convenience, weight ratios of ZLI2293/CB15/mono- and difunctional monomers were used. The mixture was ultrasonically treated to form a homogeneous solution, and then injected into an ITO glass cell separated with 15 μm spacers. The surface of the ITO substrate was pretreated with polyimide and oriented in parallel directions. To prepare PSCT cells, the sample cells with the monomer/liquid crystals mixture

TABLE I
Compositions for PSCT Cells

Sample	ZLI-2293	CB15	BAPB	BAHB	BME
A	67.9	29.1	0	2.7	0.3
B	65.96	29.1	1.94	2.7	0.3
C	64.02	29.1	3.88	2.7	0.3
D	62.08	29.1	5.82	2.7	0.3
E	72.75	0	24.25	2.7	0.3
F	67.9	0	29.1	2.7	0.3
G	63.03	0	33.97	2.7	0.3
H	58.2	0	38.8	2.7	0.3

were cured by UV irradiation with 0.65 mW/cm^2. After completing the polymerization, PSCT composite films could be fabricated. A schematic presentation of the reversed mode PSCT cells is shown in Scheme 5. Due to the surface treatment of the substrates, and pitch length of the cholesteric liquid crystal, the PSCT display device can be fabricated.

In a reverse mode PSCT, a cholesteric with a pitch of several microns is situated between two plates with homogeneous planar boundary conditions. A low concentration of a reactive monomer is dissolved in the liquid crystal. The monomer is then photopolymerized while the cholesteric is in the planar state; the resulting polymer network should thus reflect the helical structure of the planar state. The optical behaviors of the PSCT cells were investigated by using a spectrometer. The optical change of the samples induced by an electro field was monitored by detecting the intensity of the probe light transmitted through the samples with the photodiode. The intensity of the probe light in the absence of the electro field was defined as 100% light transmittance. The optical texture of the composite films was observed under crossed nicols with a polarizing microscope. The morphological observation of the solid polymer in the composite films was performed with a scanning electron microscope (SEM).

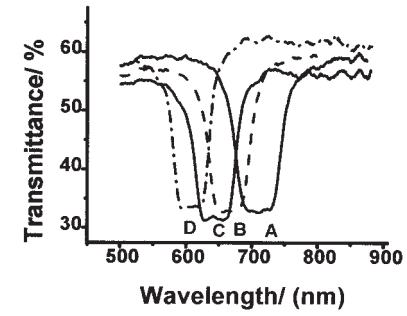

(a)

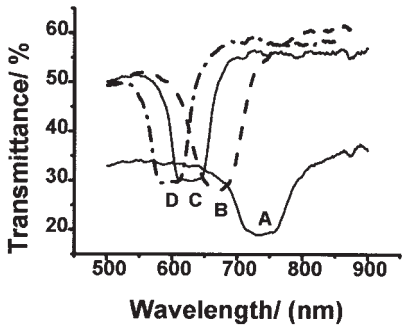

(b)

Figure 1 Reflection band of PSCT cells (a) before and (b) after UV curing.

TABLE 2
Variation on Pitch of PSCT Cells Before and After UV Curing

Cell	A	B	C	D
λ_{bef} (nm)[a)]	711	665	640	610
λ_{aft} (nm)[b)]	734	670	625	595
Shift	17	5	−15	−15
HTP	7.107	7.3	7.36	7.31
Pitch (μm)	0.469	0.4281	0.3993	0.3802

[a] Main reflection wavelength before UV irradiation.
[b] Main reflection wavelength after UV irradiation.

RESULTS AND DISCUSSION

To investigate the effects of chiral monomers derived from chiral (−)-camphor on the reflection properties of cholesteric liquid crystal cells, chiral BAPB (**7**) monomer ($[\alpha]_D = -19.1^o$) and difunctional BAHB (**10**) were synthesized as shown in Schemes 1 to 4. The molecular structures of the products were identified by using FTIR, NMR, and elemental analyses (EA). The optical rotations of the chiral compounds were also estimated using an automatic digital polarimeter with readings to ± 0.001°.

Polymer stabilized cholesteric texture (PSCT) liquid crystal cells with mixtures of nematic liquid crystals and chiral components were fabricated. Scheme 5a shows the formation of polymer stabilized cholesteric liquid crystal (PSCT) cells. After a surface coating and prerubbing, the ITO glasses were faced to each other with 15 μm spacers. The monomer/chiral nematic

TABLE 3
Variation on Pitch of PSCT Cells Before and After UV Curing

Cell	E	F	G	H
λ_{bef} (nm)[a)]	—	862	762	675
λ_{aft} (nm)[b)]	975	802	680	562
Shift		−60	−82	−113
HTP	6.42	6.5	6.576	6.96
Pitch (nm)	0.623	0.5124	0.43448	0.359

[a] Main reflection wavelength before UV irradiation.
[b] Main reflection wavelength after UV irradiation.

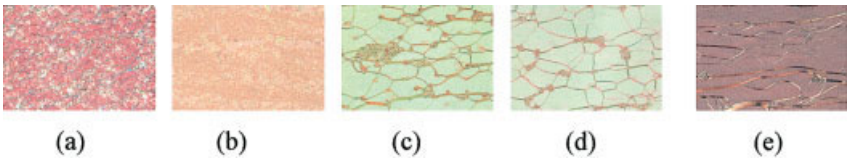

Figure 2 POM textures for PSCT cells of A, B, C, D, and E. [Color figure can be viewed in the online issue, which is available at www.interscience.wiley.com.]

mixture inside the cell was then irradiated by UV light. Photopolymerization caused the formation of polymer matrices. Due to the low polymer content in liquid crystal, a planar cell could be obtained as shown in Scheme 5a. As can be seen in Scheme 5b, the clear colored cell was changed to opaque appearance when a voltage over the threshold was applied. The orientation of liquid crystals inside the cell might be changed from planar to focal-conic, leading to the opaque refraction of incident light.[9] In this system, the polymer matrix serves two important functions. First, it influences the structure of the focal-conic state, and thus strongly influences the scattering properties of the system. Second, following the removal of the electric field, elastic forces between the polymer network and the liquid crystal cause a rapid reorientation back to the planar, nonscattering texture.

Table I shows the compositions for the preparation of polymer stabilized cholesteric texture cells. As shown in Table I, cell (A) contains no monomers. Unlike other PSCT cells, it is a cholesteric liquid crystal cell. Cells (B) to (D) contain the chiral component CB15 with chiral monomers; however, cells (E) to (H) contain only chiral monomers. The samples with the mixture of components in Table I were irradiated with UV light to fabricate PSCT cells. UV irradiation caused the polymerization of monomers, leading to the phase separation of polymers and liquid crystals. As can be seen in Figure 1 and Tables I and II, the major reflective wave length (λ_0) and the pitch of the cholesteric liquid crystal cells were changed. Sample cell numbers are indicated in the Figure. The variation of cell pitches may be due to the phase separation and differences between the chiral dopant contents in the cells. The helical twisting power (HTP) of the PSCT cells were evaluated and are summarized in Tables II and III. Higher molar contents of chiral components in the cells seemed to raise the HTP values in Table II. For cholesteric liquid crystal cell (A), as can be seen in Figure 1, UV irradiation may cause a slight degradation of liquid crystals, leading to the decay of the contrast.

Figure 2 shows the polarized optical microphotograph (POM) of PSCT cells. Figure 2a shows the texture of the cholesteric liquid crystal cell without any chiral monomer BAHB (**10**) According to theory, it can be considered as a kind of cholesteric liquid crystal in the planar texture. Figures 2b to e reveal the POM structures of PSCT cells with chiral monomers. Increasing with the chiral monomers, an oily streak on a cross section is shown in c, d, and e through an imperfect planar texture (b). The oily streak is due to the formation of interfaces between bended cholesteric areas.[9] As can be seen in Table II, chiral monomers in PSCT cells increased from cells (A) to (E). A similar texture in Figure 2e is seen although it contains no chiral component CB15. The POM texture in Figure 2e reveals that cholesteric texture is also obtained by the polymerization of the chiral monomers BAHB (**10**) in nematic liquid crystals. The texture can also be confirmed by the optical properties of the selective reflection of cell (A) in Figure 3.

Figure 4 shows the variation of the POM textures of the PSCT cell (C) affected by the applied voltage. As can be seen in Figure 3, the textures changed from planar to focal-conic. At zero field, the liquid crystal was in the planar texture with an oily streak and had a high transmittance for visible light. When the applied voltage was increased above a threshold, the liquid crystal began to tilt away from the cell plan and transfer in the polymer domains to a focal-conic texture. The dependence of the transmittance on applied voltage of the PSCT cells was estimated and summarized in Figure 4. The threshold voltage increased with an increase in the amount of polymer matrices. Higher monomer concentrations may increase the amount of

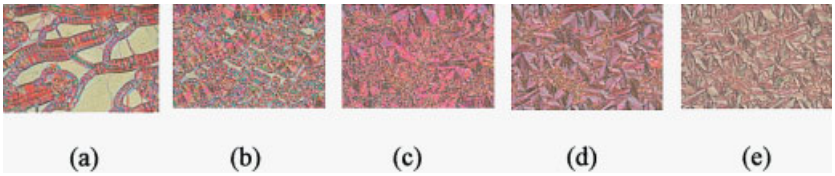

Figure 3 Texture variations of PSCT cells on applied voltage from 0 to 60 V. [Color figure can be viewed in the online issue, which is available at www.interscience.wiley.com.]

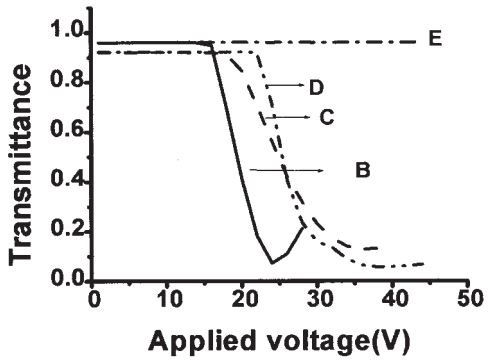

Figure 4 Dependence of transmittance of PSCT cells on applied voltage.

Figure 6 Image recording of PSCT cells through an NCKU mask with various pitches; three colors were obtained. [Color figure can be viewed in the online issue, which is available at www.interscience.wiley.com.]

polymer domains as well as the interaction forces between polymer matrices and liquid crystal molecules. Curve (E) in Figure 4 means that PSCT cell (E) did not reflect the visible light. After further investigation, selective reflection was found to exist in the infrared area.

To analyze the wavelength of the reflection of PSCT cells, the reflection spectra of the PSCT cells were studied. The results are summarized in Figure 5. A blue shift of PSCT cells was found. The results suggest that the polymerization of monomers may cause the separation of polymers and liquid crystal molecules, leading to the variation of pitches and spectra. Sample cell numbers are indicated in the Figure. As shown in Figure 5b, infrared can only be reflected for PSCT cell (E) even after UV polymerization. As illustrated in Figure 5, PSCT cell (E) did not reflect visible light.

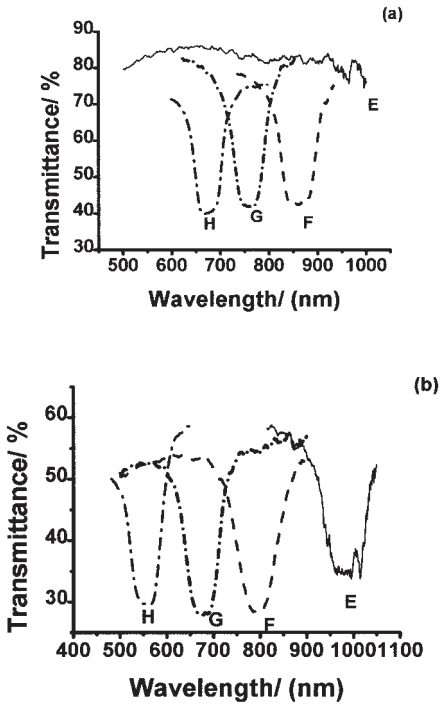

Figure 5 Reflection band of PSCT cells (a) before, and (b) after UV curing.

The pitches of the PSCT cells were calculated and summarized in Table III. The reflection main wavelength of the cell can be estimated from the following equation:

$$\lambda_0 = 2n(P_o/2) = nP_o \quad (1)$$

where λ_o is the reflection main wavelength of the PSCT cell, n is $(n_o + n_e)/2$, and P_o is the pitch of the cholesteric liquid crystal. The reflection peak is broad and has a bandwidth given by $\Delta\lambda = \Delta nP_o$, where $\Delta n = n_e - n_o$ is the birefringence. Higher monomer contents may increase the amount of polymer matrix, leading to the blue shift in Figure 5. From eq (1), a blue shift means a decreasing of cell pitches that leads to a decreasing of bandwidth. As shown in Figure 5, the reflection $\Delta\lambda$ for cell E is higher than those of the other cells.

Rear image recording of the PSCT cells was carried out, and the results are shown in Figure 6. The PSCT cells with different components were irradiated with UV light through a mask with the word NCKU. As described in Figure 5, three colors of PSCT cells were obtained. To confirm the function of voltage control on the PSCT cells, 40V a.c. power was applied on the PSCT cells. As can be seen in Figure 7, the cell was changed from transparent to opaque. The results were consistent with those described in Figure 4. The results in this investigation suggest that PSCT cells fabricated in this investigation could be applied in the field of recording materials and liquid crystal display design.

CONCLUSIONS

Chiral monomer derived from (−)-camphor and a novel difunctional monomer were synthesized. Both chiral dopant CB-15 and chiral polymers were found to form a cholesteric texture with nematic liquid crys-

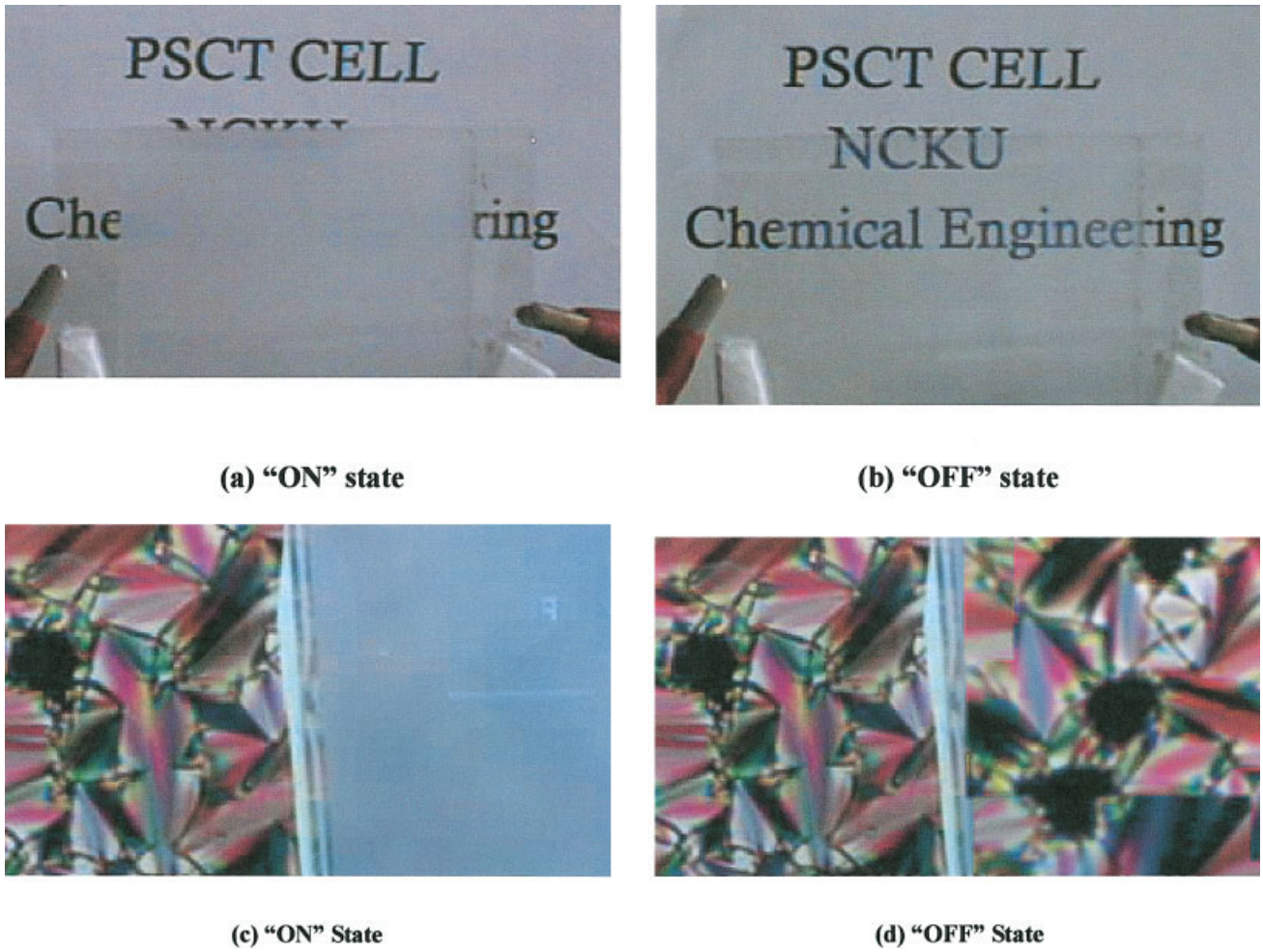

Figure 7 Representative examples of (a) and (c) "ON" state, and (b) and (d) "OFF" state of PSCT cells prepared in this investigation. [Color figure can be viewed in the online issue, which is available at www.interscience.wiley.com.]

tals. An oily streak due to the formation of interfaces between bended cholesteric areas was found by increasing the content of chiral monomers in cells. UV irradiation caused the polymerization of monomers, leading to the phase separation of polymers and liquid crystals. Higher monomer content may increase the amount of polymer matrix, leading to the results of the blue shift. PSCT cells with various components revealed different colors. The PSCT cells could also be used on displays controlled by voltage applied.

References

1. Hikmet, R. A. M.; Kemperman, H. Liq Cryst 1999, 26, 1645.
2. Li, Q.; Bai, X., Zang, J.; Tong, L. J Appl Phys 2001, 40, 6473.
3. Guillard, H.; Sixou, P.; Reboul, L.; Perichaud, A. Polymer 2001, 42, 9753.
4. Guillard, H.; Sixou, P.; Tottreau, O. Polym Adv Technol 2002, 13, 491.
5. Ren, H.; Wu, S. T. J Appl Phys 2002, 92, 797.
6. Cheng, H.; Gao, H.; Zhou, F. J Appl Phys 1999, 86, 5935.
7. Stallinga, S. J Appl Phys 1999, 86, 4756.
8. Xu, M.; Yang, D. K. Jpn J Appl Phys 2000, 38, 6827.
9. Wu, S. T.; Yang, D. K. Reflective Liquid Crystal Displays; Wiley: New York, 2001.
10. Chandrasekhar, S. Liquid Crystals; Cambridge University Press: New York, 1997; 2nd ed.
11. Pogue, R. T.; Sutherland, R. L.; Schmitt, M. G.; Natarajan, L. V.; Swecki, S. A.; Tondiglia, V. P.; Bunning, T. J Appl Spectrosc 2000, 54, 12A.
12. Yoshimoto, N.; Morino, S.; Nakagawa, M.; Ichimura, K. Opt Lett 2002, 27, 182.
13. Boyd, J. E.; Trentler, T. J.; Wahi, R. K.; Vega-Cantu, Y. I.; Colvin, V. L. Appl Opt 2000, 39, 2353.
14. Bunning, T. J.; Natarajan, L. V.; Tondiglia, V. P.; Sutherland, R. L. Annu Rev Mater Sci 2000, 30, 83.
15. Kostuk, R. K. Appl Opt 1999, 38, 1357.
16. Ren, H.; Wu, S. T. J Appl Phys 2002, 92, 797.
17. Ko, T. C.; Fan, Y. H.; Shieh, M. F.; Fuh, A. Jpn J Appl Phys Part 1 2001, 40, 2255.
18. Barchini, R.; Gordon, J. G.; Hart, M. W. Jpn J Appl Phys 1998, 37, 6662.
19. Xie, Z. L.; Kook, H. S. Jpn J Appl Phys 1998, 37, 2572.
20. Brittin, M.; Mitchell, G. R. Mol Cryst Liq Cryst 1999, 329, 145.
21. Bunning, T. J.; Natarajan, L. V.; Tondiglia, V. P. Annu Rev Mater Sci 2000, 30, 83.
22. Liu, J. H.; Tsai, F. R.; Tsai, T. Y. Polym Adv Technol 2000, 11, 228.
23. Liu, J. H.; Wang, H. Y. J Appl Polym Sci 2004, 912, 789.
24. Liu, J. H.; Wu, F. T. J Polym Res 2004, 11, 1 43.
25. Liu, J. H.; Wu, F. T. J Appl Polym Sci, to appear.